



HAL
open science

Anti-diarrheal drug loperamide induces dysbiosis in zebrafish microbiota via bacterial inhibition

Rebecca Stevick, Sébastien Bedu, Nicolas Dray, Jean-Marc Ghigo, David Pérez-Pascual

► **To cite this version:**

Rebecca Stevick, Sébastien Bedu, Nicolas Dray, Jean-Marc Ghigo, David Pérez-Pascual. Anti-diarrheal drug loperamide induces dysbiosis in zebrafish microbiota via bacterial inhibition. *Microbiome*, 2023, 11, pp.252. 10.1186/s40168-023-01690-z . pasteur-04253857v2

HAL Id: pasteur-04253857

<https://pasteur.hal.science/pasteur-04253857v2>

Submitted on 12 Nov 2024

HAL is a multi-disciplinary open access archive for the deposit and dissemination of scientific research documents, whether they are published or not. The documents may come from teaching and research institutions in France or abroad, or from public or private research centers.

L'archive ouverte pluridisciplinaire **HAL**, est destinée au dépôt et à la diffusion de documents scientifiques de niveau recherche, publiés ou non, émanant des établissements d'enseignement et de recherche français ou étrangers, des laboratoires publics ou privés.



Distributed under a Creative Commons Attribution 4.0 International License

RESEARCH

Open Access



Anti-diarrheal drug loperamide induces dysbiosis in zebrafish microbiota via bacterial inhibition

Rebecca J. Stevick¹, Bianca Audrain¹, Sébastien Bedu², Nicolas Dray², Jean-Marc Ghigo^{1*} and David Pérez-Pascual^{1*}

Abstract

Background Perturbations of animal-associated microbiomes from chemical stress can affect host physiology and health. While dysbiosis induced by antibiotic treatments and disease is well known, chemical, nonantibiotic drugs have recently been shown to induce changes in microbiome composition, warranting further exploration. Loperamide is an opioid-receptor agonist widely prescribed for treating acute diarrhea in humans. Loperamide is also used as a tool to study the impact of bowel dysfunction in animal models by inducing constipation, but its effect on host-associated microbiota is poorly characterized.

Results We used conventional and gnotobiotic larval zebrafish models to show that in addition to host-specific effects, loperamide also has anti-bacterial activities that directly induce changes in microbiota diversity. This dysbiosis is due to changes in bacterial colonization, since gnotobiotic zebrafish mono-colonized with bacterial strains sensitive to loperamide are colonized up to 100-fold lower when treated with loperamide. Consistently, the bacterial diversity of gnotobiotic zebrafish colonized by a mix of 5 representative bacterial strains is affected by loperamide treatment.

Conclusion Our results demonstrate that loperamide, in addition to host effects, also induces dysbiosis in a vertebrate model, highlighting that established treatments can have overlooked secondary effects on microbiota structure and function. This study further provides insights for future studies exploring how common medications directly induce changes in host-associated microbiota.

Keywords Zebrafish, Microbiota, Host-microbe system, Dysbiosis, Loperamide, Colonization, Antibacterial activity

*Correspondence:

Jean-Marc Ghigo

jmghigo@pasteur.fr

David Pérez-Pascual

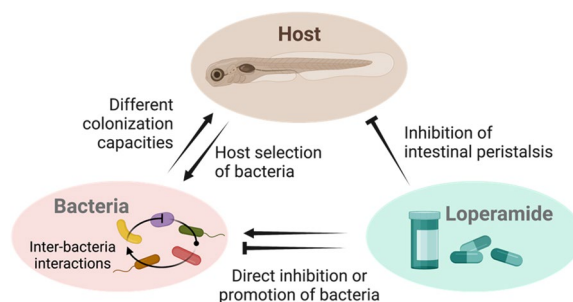
dperezpascu@gmail.com

Full list of author information is available at the end of the article



© The Author(s) 2023. **Open Access** This article is licensed under a Creative Commons Attribution 4.0 International License, which permits use, sharing, adaptation, distribution and reproduction in any medium or format, as long as you give appropriate credit to the original author(s) and the source, provide a link to the Creative Commons licence, and indicate if changes were made. The images or other third party material in this article are included in the article's Creative Commons licence, unless indicated otherwise in a credit line to the material. If material is not included in the article's Creative Commons licence and your intended use is not permitted by statutory regulation or exceeds the permitted use, you will need to obtain permission directly from the copyright holder. To view a copy of this licence, visit <http://creativecommons.org/licenses/by/4.0/>. The Creative Commons Public Domain Dedication waiver (<http://creativecommons.org/publicdomain/zero/1.0/>) applies to the data made available in this article, unless otherwise stated in a credit line to the data.

Graphical Abstract



Background

Animal-associated microbiomes are dynamic communities that play essential roles in the physiology, health, and evolution of their hosts [1]. Numerous studies have explored the impact of different phenomena on microbiota stability, including antibiotic treatments, gut health, or environmental factors, in order to understand the consequences of microbiota perturbations on host functions [2–5]. These perturbations may lead to dysbiosis or a change in microbial community composition and/or function, relative to the steady state, with potential implications for host health [6, 7].

While the complexity of microbiota in humans and animal models limits functional and mechanistic studies, germ-free and gnotobiotic animal models with controlled, tractable microbiota are widely used to study host-microbiota interactions [8]. Compared to conventional animals with relatively variable microbiota [9], gnotobiotic animals with host-specific bacterial consortia can mimic key phenotypes for mechanistic studies and are powerful tools to simplify microbiota and increase experimental reproducibility [10]. In particular, zebrafish (*Danio rerio*), which possesses both an innate and adaptive immune system and a mammal-like intestinal epithelium, has emerged as an established gnotobiotic model to study vertebrate host-microbiota interactions [11, 12]. Gnotobiotic larval zebrafish can indeed be easily reared to study simplified host-microbial systems in the context of developmental biology, immunology, and disease [13, 14].

Loperamide is a prevalent medication for treating diarrhea in humans and animals that acts on μ -opioid receptors in the large intestine, decreasing intestinal peristaltic activity and increasing the absorption of fluids [15–18]. Loperamide is also used to study bowel dysfunction and constipation in animal models, including rats, mice, and zebrafish, generating a relevant model of irritable bowel syndrome or opioid-induced bowel dysfunction disorder

[19–21]. In zebrafish, loperamide treatment was shown to cause a significant decrease in intestinal peristaltic frequency that can be restored by the presence of specific bacteria or acetylcholine [21, 22].

Despite its pervasive use in humans and animal models, the potential effects of loperamide on host-associated microbiota in vitro and in vivo are poorly characterized. It has been suggested that slow transit time and constipation induced by loperamide could be responsible for changes in bacterial composition and decreased diversity observed in rats and mice [23–26]. Although publications using loperamide to investigate host-associated microbiota establish the link between constipation and microbial dysbiosis, recent studies have identified loperamide hydrochloride and its derivatives as molecules displaying bactericidal activity [27–29]. Hence, the extent of microbial dysbiosis directly caused by this compound versus its impact on the alteration of host function is poorly understood and ignored in animal models.

In this study, we used conventional and gnotobiotic larval zebrafish to reproduce in vivo loperamide-induced dysbiosis based on in vitro bacterial sensitivity to loperamide. We found that loperamide leads to recoverable dysbiosis in conventional larval zebrafish according to strain-specific inhibition or promotion of bacteria. Our results demonstrate how a relevant chemical perturbation induces dysbiosis in a vertebrate microbiome model. These findings should be considered in the context of secondary effects of established treatments, assumed mode of action in animal models, and microbiota recovery.

Methods

General zebrafish husbandry

Wild-type AB/AB zebrafish (*Danio rerio*) fertilized eggs at 0 day post fertilization (dpf) were obtained from the ZorqI'hub platform at Institut Pasteur. All procedures were performed at 28 °C under a laminar microbiological hood with single-use disposable plasticware according

to European Union guidelines for handling of laboratory animals and were approved by the relevant institutional Animal Health and Care Committees. Eggs were kept in 25 cm³ vented flasks (Corning 430,639) with 20 mL of autoclaved mineral water (Volvic) until 4 dpf (30–33 eggs/flask) and transferred to new flasks after hatching at 4 dpf (10–15 fish/flask). At 6 dpf, each fish was transferred to an individual well of a 24-well plate (TPP 92024) in 2 mL of autoclaved mineral water and maintained until the end of the experiment (11 dpf). Conventional zebrafish embryos were transferred to flasks at 1 dpf and maintained as described. At the end of the experiment, zebrafish were euthanized with an overdose of tricaine (MS-222, Sigma-Aldrich E10521) at 0.3 mg/mL for 10 min.

Fish were fed with sterile *Tetrahymena thermophila* every 48 h starting at 4 dpf. Germ-free *T. thermophila* stocks were kept in 15 mL of PPYE broth (0.25% protease peptone BD Bacto no. 211684, 0.25% yeast extract BD Bacto no. 212750) supplemented with penicillin G (10 unit/mL) and streptomycin (10 µg/mL) at 28 °C. Every week, a new stock was inoculated with 100 µL of the previous stock and tested for sterility on LB, TYES, and YPD agar media plates. To prepare food for the zebrafish, *T. thermophila* was inoculated at a 1:50 ratio from the stock into 20-mL MYE broth (1% milk powder, 1% yeast extract) and grown for 2 days. On feeding day, the *T. thermophila* was transferred to a 50-mL Falcon tube and washed 3 times (4400 rpm, 3 min at 28 °C) with sterile mineral water. Resuspended *T. thermophila* was added to the fish in culture flasks (500 µL in 20 mL) or 24-well plates (50 µL in 2 mL).

Germ-free zebrafish sterilization

The zebrafish embryos were sterilized as previously described with the following modifications [13, 30]. Recently, fertilized zebrafish eggs (0 dpf) were bleached (0.000005% final v/v) for 5 min and then washed 2 times in sterile mineral water. Eggs were then maintained in 50-mL Falcon tubes (100 eggs/tube) overnight in 35 mL of sterile mineral water supplemented with 0.4 µg/mL methylene blue solution (Sigma Aldrich 50,484). At 1 dpf, the volume of each tube was adjusted to 50 mL, and the eggs were treated with an antibiotic cocktail for 2 h with gentle agitation at 10 rev/min: penicillin G:streptomycin at 100 µg/mL (GIBCO 15140148), kanamycin sulfate at 400 µg/mL (PAN-Biotech P06-04010P), and amphotericin B solution at 250 µg/mL (Sigma-Aldrich A2942). Then, the eggs were washed 3 times with sterile mineral water and resuspended in 50-mL water. The eggs were bleached (0.000005% final v/v) for 15 min with inversion every 3 min and then washed 3 times in sterile mineral water and resuspended in 50-mL water. Finally, the eggs

were treated with 1% Romeoid solution (COFA, France) for 10 min and then washed 3 times in sterile mineral water. Eggs were then transferred to 25 cm³ vented flasks and maintained as described above.

Sterility was confirmed at 3 dpf by spotting 50 µL of water from each flask on LB, TYES, and YPD agar plates and incubated at 28 °C under aerobic conditions for at least 3 days. In addition, monthly checks of bacterial contamination were done by PCR amplification of water samples with 16S rRNA gene primers as described below in the characterization section. Contaminated flasks were immediately removed from the experiment and not included in the results.

Generation of gnotobiotic zebrafish

Germ-free zebrafish larvae were colonized at 4 dpf, as follows. Overnight cultures of a single bacterial colony in 5 mL of liquid media were washed twice with sterile mineral water and normalized to OD 0.1 in water. For mono-colonization, 200 µL of bacterial suspension was added into flasks of germ-free zebrafish in 20 mL of sterile mineral water at a final concentration of 5 × 10⁵ CFU/mL. For mix5 colonization, 200 µL of each strain was added per flask at a final concentration of 5 × 10⁵ CFU/mL per strain. Water samples were plated in serial dilutions to confirm final bacterial concentration and sterility. Bacterial exposure was performed for 48 h until fish were transferred to sterile water in 24-well plates.

Zebrafish loperamide treatment

Loperamide hydrochloride (Sigma-Aldrich 34,014) was dissolved in pure dimethyl sulfoxide (DMSO, Sigma-Aldrich D8418) at a stock concentration of 100 mg/mL. Larval zebrafish were treated at 5 dpf with loperamide at a final concentration of 10 mg/L in 20-mL vented flasks for 24 h, which has been previously shown to significantly reduce peristaltic movement in larval zebrafish at 4–6 dpf [21]. Sterile DMSO added at a final concentration of 1:10,000 was used as the control. After 24 h of treatment, all 6 dpf fish were transferred to water and maintained until sampling.

Conventional zebrafish sampling and DNA extraction

Zebrafish larvae were sampled at each of 3 timepoints (6 dpf, 7 dpf, 11 dpf) with 3 treatment conditions (control water, DMSO 1:10,000, loperamide 10 mg/L) as follows. At each timepoint, 5 larval fish per condition (15 total) were washed twice by transfers to clean, sterile water to remove environmental and residual bacteria. Each fish was then added to a sterile 2-mL microcentrifuge tube in 200 µL of water and euthanized with tricaine at 0.3 mg/mL. All liquid was removed from the tissue, and then the

samples (45 total) were immediately frozen at -80°C and stored until DNA extraction.

DNA extraction was performed from single larval zebrafish using the DNeasy Blood & Tissue Kit (Qiagen 69,504) with modifications as follows. Tissue samples were thawed at room temperature, and then 380- μL Buffer ATL and 20- μL proteinase K were added directly to each individual larva in a 2-mL tube. Samples were vortexed for 15 s and then incubated overnight (15–18 h) until fully lysed at 56°C and 300 rpm using a shaker-incubator (Eppendorf ThermoMixer C). After lysis, 4 μL of RNase A solution was added, and the samples were incubated for 5 min at room temperature to remove residual RNA. Next, 400- μL Buffer AL and 400- μL 100% ethanol were added and mixed by vortexing before loading the lysate onto the DNeasy mini spin column in 2×600 μL loads. DNA purification and clean-up proceeded according to the manufacturer's recommendations with a final elution volume of 50 μL in Buffer AE. Purified DNA was quantified using the Qubit HS DNA fluorometer kit (ThermoFisher Q32851), and purity was assessed with the NanoDrop spectrophotometer (ThermoFisher). DNA yields per single fish sample ranged from 10 to 15 ng/ μL in 50 μL with purity ratios >1.8 . Negative controls for the extraction kit were prepared alongside zebrafish samples, but with no tissue input.

Conventional fish 16S rRNA gene amplicon sequencing and analysis

16S rRNA gene amplicons of the V6 region for the 45 conventional zebrafish samples, 2 mock community samples (Zymo Research DNA standard I D6305), 2 negative DNA extraction samples, and blank PCR control were prepared using 967F/1064R primers. The DNA extraction negative control samples were pooled and concentrated prior to PCR to obtain enough product for sequencing. A two-step PCR reaction using 200 ng of zebrafish DNA was performed in duplicate 50- μL reactions as previously described [31, 32]. Each first step reaction included 25- μL 2X Phusion Mastermix (Thermo Scientific F531S), 1.5 μL of 10- μM F/R primer mix (967F: CTAACCGANGAACCTYACC, CNACGCGAAGAACC TTANC, CAACGCGMARAACCTTACC, ATACGCGAR GAACCTTACC (equimolar mix)/1064R: CGACRCCA TGCANCACCT), 13–20 μL template DNA (200 ng), and 3.5–10.5 μL nuclease-free water (up to 50 μL). PCR amplification (step 1) conditions were denaturing at 98°C for 3 min followed by 30 cycles of denaturation at 98°C for 10 s, primer annealing at 56°C for 30 s, extension at 72°C for 20 s, and then a final extension at 72°C for 20 s. Negative controls for the PCR reagents were prepared alongside zebrafish DNA samples but with additional nuclease-free water input. PCR products were

assessed for concentration (Qubit DNA HS reagents) and expected size using agarose gel electrophoresis. A second PCR step was performed to attach sequencing barcodes and adaptors according to Illumina protocols. The PCR products were analyzed with 250-bp paired-end sequencing to obtain overlapping reads on an Illumina MiSeq at the Institut Pasteur Biomics platform.

The resulting 16S rRNA gene amplicon sequences were demultiplexed and quality filtered using DADA2 (v1.6.0) implemented in QIIME2 (v2020.11.1) with additional parameters $-p\text{-trunc-len-r } 80 -p\text{-trunc-len-f } 80 -p\text{-trim-left-r } 19 -p\text{-trim-left-f } 19$ to determine amplicon sequence variants (ASVs) [33, 34]. All ASVs were summarized with the QIIME2 pipeline (v2020.11.1) and classified directly using the SILVA database (99% similarity, release no. 134) [35, 36]. Processed ASV and associated taxonomy data were exported as a count matrix for analysis in R (v4.1.3). The positive and negative controls were checked to ensure sequencing quality and expected relative abundances. Nonbacterial and chloroplast sequences were then removed by taxonomic ASV calls where Kingdom = "d__Eukaryota", Kingdom = "d__Archaea", and Phylum = "Cyanobacteria". Finally, the data was normalized by percentage to the total ASVs in each sample for further dissimilarity metric analysis.

All descriptive and statistical analyses were performed in the R statistical computing environment with the *tidyverse* v1.3.1, *vegan* v2.5.7, and *phyloseq* v1.38.0 packages [37–39]. Rarefaction curves and sequencing coverage estimates were generated using the `rarecurve()` commands with `sample=[number of reads in smallest sample]` in *vegan* v2.5.7 [40]. Nonmetric dimensional analysis (NMDS) was used to determine the influence of timepoint or loperamide treatment on the ASV-level composition. The Bray–Curtis dissimilarity metric was calculated with $k=2$ for max 50 iterations, and 95% confidence intervals (standard deviation) were plotted. Statistical testing of the beta-diversity was done using the PERMANOVA *adonis2* test implemented in *vegan* (method = "bray," $k=2$) [41, 42]. Within-condition variability was calculated using the command `vegdist` (method = "bray," $k=2$), and the matrix was simplified to include samples compared within each timepoint.

Significant differences in genera between DMSO (reference) and loperamide treated (test) at each timepoint were calculated using *limma* implemented in the *microbiomeMarker* v1.1.2 package using the following conditions: `norm="RLE," pvalue_cutoff=0.05, taxa_rank="Genus,"` and `p_adjust="fdr"` [43–45]. Simpson's diversity values were calculated for each sample at the ASV level using the *vegan* package and analyzed using the nonparametric Kruskal–Wallis rank-sum test in R. Additional visualizations were computed using the

ComplexHeatmap v2.10.0 and *UpSetR* v1.4.0 packages [46, 47]. All processed sequencing files, bash scripts, QIIME2 artifacts, and Rmd scripts to reproduce the figures in the manuscript are available on Zenodo [48].

Measurement of zebrafish growth and development

In order to determine the effect of loperamide growth on larval fish growth and development, 9–10 fish were sampled at each timepoint (6, 7, 11 dpf) for each condition (control water, DMSO, loperamide)=85 fish total. After euthanasia, the samples were fixed in 1% paraformaldehyde (PFA) and stored at 4 °C. After fixation, the samples were rinsed 3 times with PBS and then placed into individual wells in a plate. Microscopy images were taken with a Leica M80 10X with a Leica IC80 HD camera. Four images were captured per sample: whole at 2.5X, caudal at 5X, lateral at 5X, and head at 5X for a total of 337 images for 85 samples. Relevant measurements of each fish sample were performed using ImageJ [49]. Four measurements in millimeters were taken per fish: eye diameter, rump-anus length, standard length, and tail width according to methods previously described [50–52].

Bacterial strains and growth conditions

Bacterial strains are listed in Supplementary Table S1. Zebrafish-associated strains were grown in tryptone yeast extract salts (TYES) or Miller's Lysogeny Broth (LB) (Corning) and incubated at 28 °C with rotation. Cultures on solid media were on LB or TYES with 1.5% agar. Bacteria were always streaked from glycerol stocks on LB or TYES agar before inoculation with a single colony in liquid cultures. All media and chemicals were purchased from Sigma-Aldrich.

Isolation and 16S characterization of bacteria from conventional zebrafish

Five of the zebrafish-associated strains were previously isolated and characterized from the zebrafish environment [53]. The following strains were isolated and identified in the same way in this study: S2, S4, S8, and S9. Zebrafish lysates and tank water were serially diluted and plated on R2A, TYES, and LB agar and incubated at 28 °C for up to 3 days. Each colony morphotype per media was catalogued and re-streaked on the same agar. The morphotype identification was done as previously described [53, 54]. Individual colonies were picked for each morphotype from each agar plates, vortexed in 200- μ L DNA-free water, and boiled for 10 min at 90 °C. Five microliters of this bacterial suspension was used as template for colony PCR to amplify the 16S rRNA gene with the universal primer pair 27f and 1492R. 16S rRNA gene PCR products were verified on 1% agarose gels, purified with the

QIAquick PCR purification kit (Qiagen), and two PCR products for each morphotype were sent for sequencing (Eurofins, Ebersberg, Germany). Individual 16S rRNA-gene sequences were compared with those available in the EzBioCloud database [55]. Species-level identification which was performed based on the 16S rRNA gene sequence similarity was >99%. The zebrafish-associated strains used in this study (Table S1) were chosen from this catalogue based on their sensitivity to loperamide and match with significant changes in the conventional 16S rRNA gene amplicon data.

Bacterial growth curves and survival assays

Overnight cultures of a single bacterial colony in 5 mL of liquid media were measured and normalized to OD 0.5. Liquid media supplemented with 10 mg/L loperamide in DMSO or 1:10,000 DMSO or control was added to a TPP flat-bottom polystyrene 96-well plate. Bacterial cultures were added to each condition in triplicate at a final starting concentration of OD 0.05 in 100 μ L. Negative control wells were included for each media and condition. A plastic adhesive film (adhesive sealing sheet, Thermo Scientific, AB0558) was used to seal the wells, and the plates were then incubated in a TECAN Infinite M200 Pro spectrophotometer for 20 h at 28 °C. OD600 was measured every 30 min, after a 30-s orbital shaking of 2-mm amplitude.

Bacterial survival in water was tested using the in vivo colonization conditions described above. Overnight cultures of a single bacterial colony in 5 mL of liquid media were washed twice with autoclaved Volvic water and measured and normalized to OD 0.1 in water. Bacteria were inoculated at a final concentration of 5×10^5 CFU/mL into 10 mL of Volvic water supplemented with loperamide in DMSO at 10 mg/L or 1:10,000 DMSO or control. Viable colony-forming units (CFUs) were counted from each flask at 0, 6, 24, 48, and 72 h as follows. Three \times 200- μ L aliquots were sampled, and dilutions were made, and then 10- μ L drops were plated on LB or TYES and grown at 28 °C for 2 days. CFUs were then counted for each strain, and CFUs/mL were calculated by $1000 \mu\text{L}/\text{mL}/10 \mu\text{L plated} \times \text{dilution factor} \times (\text{average of replicate CFUs per strain})$. Survival of each strain was repeated at least two independent times.

Quantification of gnotobiotic zebrafish bacterial load by CFU counts

Zebrafish were sampled at each of 3 timepoints (6 dpf, 7 dpf, 11 dpf) with 3 treatment conditions (control water, DMSO 1:10,000, loperamide 10 mg/L). At each timepoint, 3–4 larval fish per condition were washed twice by 2 transfers to clean, sterile water in petri dishes to remove environmental and residual bacteria. The larvae were

then euthanized with tricaine at 0.3 mg/mL and added in 500 µL of sterile water to 2-mL tubes containing 1.4-mm ceramic beads (Fisher Scientific 15,555,799). Fish were homogenized for 2×45 s at 6000 rpm using a 24 Touch homogenizer (Bertin Instruments). These homogenization conditions are sufficient to lyse zebrafish tissue, but not harmful to the bacteria. The lysate was then diluted from 10- to 100-fold. For the mono-colonized fish, 10-µL drops were plated in triplicate for each dilution on media. After 2 days of incubation at 28 °C, CFUs were counted, and CFUs per fish were calculated by 500-µL lysate/100 µL plated×dilution factor×average of replicate CFUs. For the mix5-colonized fish, 3×100 µL from each dilution was spread on media using sterile glass beads to differentiate the colonies. After 2 days of incubation at 28 °C, CFUs were counted for each strain, and CFUs per strain per fish were calculated by 500-µL lysate/100 µL plated×dilution factor×(average of replicate CFUs per strain).

Statistical analyses

All plotting and statistical analyses were performed in the R statistical computing environment (4.1.3) using RStudio (v.2022.02.1) with the *tidyverse* v1.3.1, *ggpubr* v0.4.0, *ggtext* v0.1.1, and *patchwork* v1.1.1 packages [39, 56–58]. Nonparametric global Kruskal–Wallis tests and subsequent Wilcoxon pairwise tests were performed to compare loperamide-treated condition to the DMSO control using *compare_means()* or *stat_compare_means()* when *p*<0.05 is significant. For the comparison of zebrafish colonization and water survival, mean CFUs/mL or CFUs/fish of each strain S1–S10 were calculated for control conditions at 48 h or T0, respectively. The colonization efficiency for each strain was calculated by

$colonization\ efficiency = \frac{mean\ CFUs\ per\ fish}{mean\ water\ CFUs\ per\ mL} \times 100$. The correlation between the variables was fit with *geom_smooth(method="lm")*, and the fit was indicated with correlations using *stat_cor()* and *stat_regline_equation()*. Hypothetical bacterial composition comparison of mono-colonized fish was calculated by the mean CFUs per fish per strain/the sum of mean CFUs per fish of S1, S3, S5, S6, and S7. Bacterial composition comparison of mix5-colonized fish was calculated by the mean CFUs of each strain/the total CFUs of all strains in each fish. Simpson’s diversity values were calculated for each mix5-colonized fish based on percent abundance per strain using the *vegan* package and analyzed using the nonparametric Kruskal–Wallis rank-sum test in R. All raw data and Rmd scripts to reproduce the figures and statistical tests in the manuscript are available on Zenodo [48].

Results

Loperamide treatment induces recoverable dysbiosis in conventional larval zebrafish microbiota

Using the experimental procedure described in Fig. 1, we determined the impact of loperamide treatment on conventional larval zebrafish microbiota using 16S rRNA gene amplicons sequenced from whole fish samples after 24 h of treatment (T0), 24 h of recovery (T1), and 5 days of recovery (T5). A total of 2,161,882 quality-controlled, bacterial 16S rRNA gene amplicon sequences were analyzed from 45 larval zebrafish samples (Fig. S1A). Sequence variant analysis using QIIME2 and taxonomic classification resulted in the detection of 1186 bacterial genera across 39 phyla to sufficiently cover the estimated high diversity in the samples (Fig. S1B). A sequenced mock bacterial community yielded similar proportions

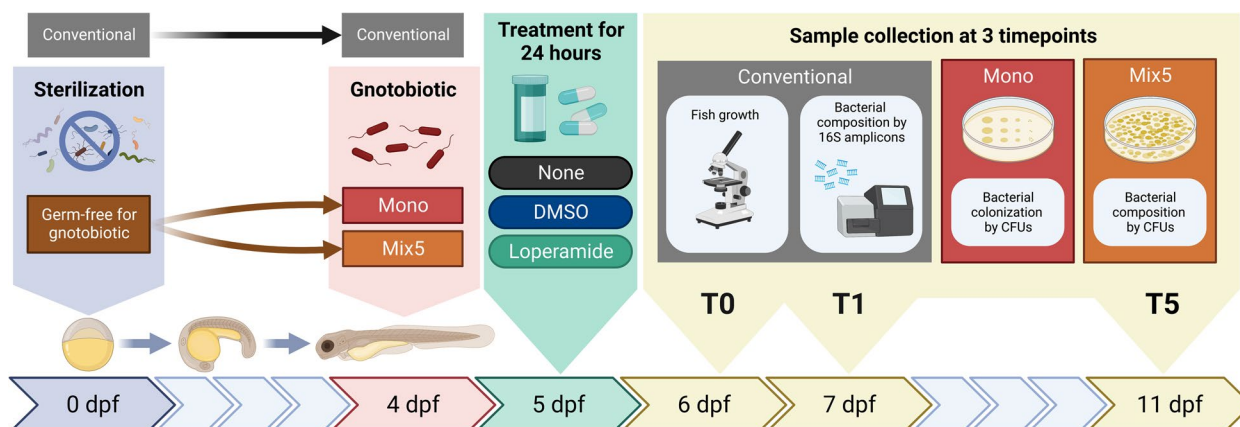


Fig. 1 Experimental scheme of the larval zebrafish assays and sample collection. Conventional, mono-colonized, or mix5-colonized larval zebrafish were exposed at 5 dpf to water (control), DMSO (control) or 10 mg/L loperamide hydrochloride (treated) for 24 h and then transferred to water at 6 dpf. Samples were collected at 6 dpf, 7 dpf, and 11 dpf (T0, T1, T5) to measure fish growth and quantify bacterial community composition in all conditions (dpf, days post fertilization; CFUs, colony-forming units)

as the expected positive control (Fig. S2AB). Additionally, blank negative control samples from the DNA extraction and PCR steps were analyzed (Fig. S2C). The ASVs detected in the negative controls were relatively low in the zebrafish samples, confirming the absence of contamination. Proteobacteria was the dominant phylum in the larval zebrafish microbiota comprising $75 \pm 17\%$ of the samples, followed by Bacteroidota ($9.6 \pm 9.2\%$) and Firmicutes ($5.0 \pm 13\%$) (Fig. S3; values averaged across all samples). The largest group of 100 shared genera was common to all DMSO and loperamide samples, regardless of timepoint or treatment (Fig. S4B; black bar).

Differences in the conventional zebrafish bacterial community composition were observed between the timepoints and treatment (Figs. 2, S3, S4, and S5). At T0 and

T1, the beta-diversity of loperamide-treated fish microbiota was significantly different from the DMSO control (Fig. 2A, S5B [adonis2 PERMANOVA $R^2=0.43$; $p<0.01$], S5C [adonis2 PERMANOVA $R^2=0.51$; $p<0.01$]). However, after 5 days of recovery (T5), the DMSO and loperamide-treated fish microbiota composition were not significantly different, indicating a recovery of microbiota composition once the treatment ended (Fig. 2A, Fig. S5D [adonis2 PERMANOVA $R^2=0.22$; $p>0.05$]). This recoverable dysbiosis in microbiota composition induced by loperamide treatment was driven by a decrease in genus *Ensifer* and an increase in genus *Aeromonas* at T0 (Figs. 2B, S4A). At T1, there were major significant differences, affecting 37 different taxonomic groups; 6 of them with >1% abundance: a 4-log decrease in *Acidovorax* and

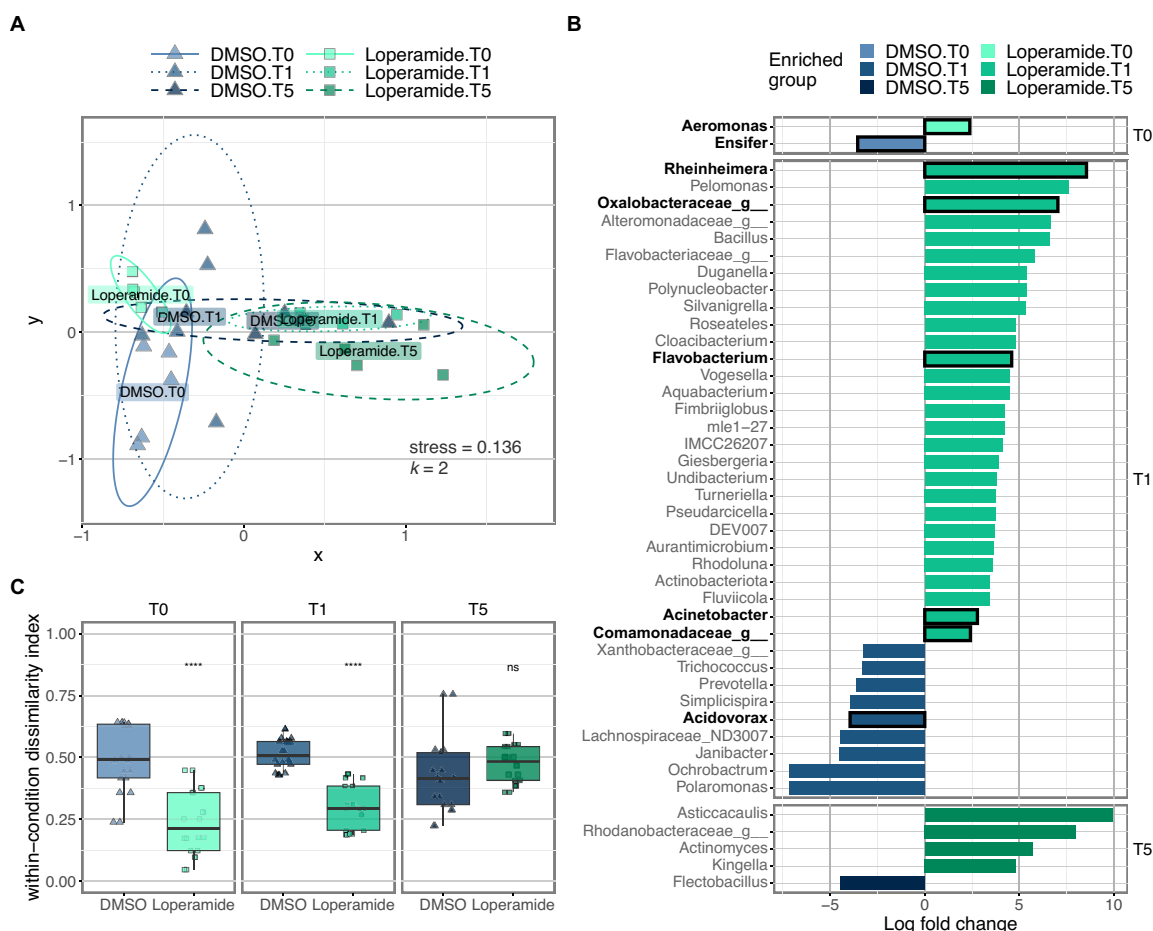


Fig. 2 Loperamide affects conventional zebrafish microbiota as measured by 16S rRNA gene amplicons. **A** NMDS plot calculated using Bray–Curtis beta-diversity ($k=2$) of percent normalized ASVs from 16S rRNA gene amplicons. Ellipse lines show the 95% confidence interval (standard deviation). Stress = 0.136; adonis2 PERMANOVA $R^2=0.104$; $p=0.029^*$. Only DMSO and loperamide-treated samples are shown. **B** Significant differentially abundant genera in loperamide-treated fish, compared to DMSO controls at each timepoint calculated using Limma (one against one) with conditions: relative log expression (RLE) normalized, effect log fold change > 2, Benjamini and Hochberg adjusted p -value < 0.05 ($n=5$ per condition). Genera that occur at mean percent abundance > 1% are outlined in black and bold. **C** Beta-dispersion or within-condition dissimilarity index calculated using Bray–Curtis beta-diversity ($n=20$). **** $p<0.001$ for loperamide treatment, compared to DMSO. Wilcoxon test

significant enrichment of Comamonadaceae, *Acinetobacter*, *Flavobacterium*, Oxalobacteraceae, and *Rheinheimera* taxa (Fig. 2B). After 5 days of recovery at T5, there were no significantly different genera that were >1% abundant in the conventional zebrafish (Fig. 2B). Loperamide treatment also resulted in significantly decreased within-group beta-diversity compared to the DMSO control at T0 and T1, but not T5 (Fig. 2C). Despite the differences in bacterial composition and treatment regimen, overall growth and development of conventional zebrafish were not affected by loperamide treatment (Fig. S6). Eye diameter, but not fish length, tail width, or rump-anus length, was significantly smaller at T5 in loperamide-treated conditions (Fig. S6D).

Members of the conventional zebrafish community are inhibited or promoted by loperamide in vitro

Based on the changes observed in the conventional zebrafish bacterial community, 9 strains isolated from the zebrafish environment (conventional larvae or rearing water) and a *Flavobacterium* spp. were tested for their sensitivity to loperamide in vitro (Table S1). When grown in rich media in the presence of loperamide, the growth of 8/10 strains was significantly affected, while S2 *Variovorax gossypii* and S3 *Pseudomonas nitroreducens* were not affected (Fig. S7). One strain (S1 *Pseudomonas mosselii*) showed increased growth rate and carrying capacity in the presence of loperamide, compared to DMSO control. All other affected strains (7/10) showed no growth, delayed growth, slower growth rates, or reduced carrying

capacity when grown in media supplemented with loperamide (Fig. S7). In addition to growth, survival in water according to in vivo conditions was tested for the 10 strains by counting daily CFUs for 3 days of incubation. Survival of 6 out of 10 strains was not significantly affected by loperamide in these conditions: S1, S4, S5, S6, S9, and S10 (Fig. 3). Three strains (S2, S3, S8) showed increased survival in the presence of loperamide, while S7 *Aeromonas veronii* was the only strain with significantly inhibited survival at 24 h.

Individual bacterial colonization of mono-colonized larval zebrafish is strain specific and affected by loperamide

In order to test the zebrafish colonization capacity of bacteria and the loperamide effects in vivo, 10 bacterial strains were individually added to colonize GF fish and then sampled at T0, T1, and T5 for whole fish CFU counts. All bacterial strains colonized the zebrafish in control conditions at 6 dpf after 2 days of exposure at 10^3 to 10^6 CFUs per larvae (Fig. 4A). S4 *Achromobacter marplatensis* had the highest bacterial colonization capacity at a mean of 2.2×10^5 CFU/fish, while the bacterial load of larvae colonized with non-autochthonous S10 *Flavobacterium johnsoniae* was only 4.6×10^3 CFU/fish. Overall bacterial colonization of the zebrafish was on average 10- to 100-fold lower than the number of CFUs per milliliter in the water at this time with colonization efficiencies of 0.7–52% (Fig. S8A). Strain S7 *A. veronii* displayed the highest colonization efficiency with a mean of 1.1×10^5 CFUs/mL in the water, compared to 5.9×10^4

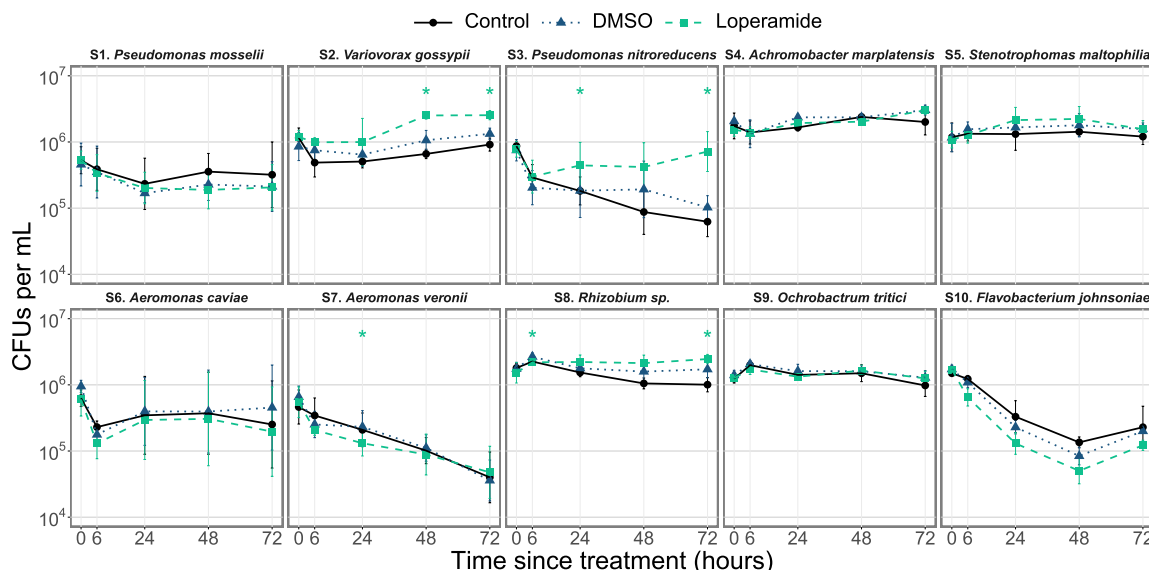


Fig. 3 In vitro survival in water of zebrafish-associated bacterial strains is affected by loperamide. Survival in water for 72 h after inoculation at 10^6 CFUs/mL (mean \pm standard deviation per condition is shown, $n=6-12$; 2–4 independent assays of 3 biological replicates). * $p < 0.05$ for loperamide treatment, compared to DMSO. Wilcoxon test. Note log scale on y-axis

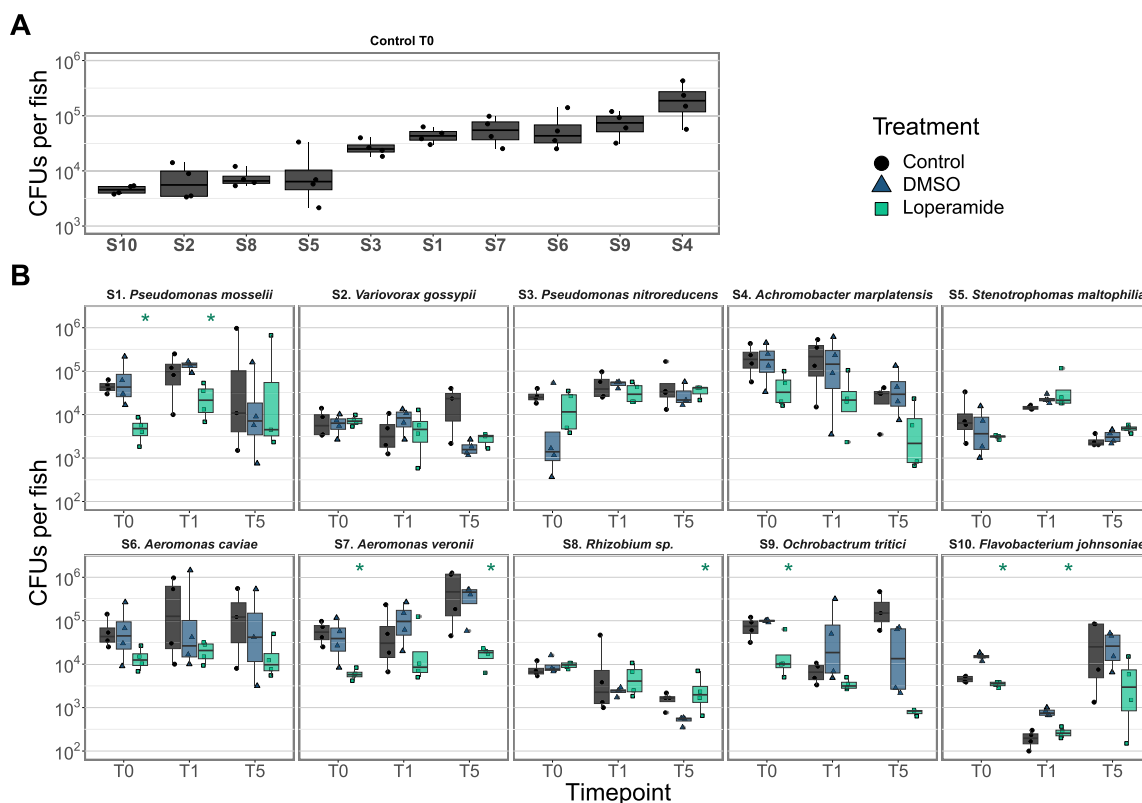


Fig. 4 Loperamide can increase or reduce zebrafish mono-colonization. CFUs per fish of mono-colonized fish in **A** control conditions at T0 (6 dpf) ordered by colonization capacity and **B** after exposure to loperamide at 3 timepoints ($n=4$ fish). Each point represents a single zebrafish (mean of 3 technical replicates). * $p < 0.05$ for loperamide treatment, compared to DMSO. Wilcoxon test. Note log scale for y-axis

CFUs per fish (efficiency = 52.9%). Conversely, strains S8, S5, and S2 had colonization efficiencies of ~ 1% with ~ 10^6 CFUs/mL in the water, compared to ~ 10^4 CFUs per fish (Fig. S8A). Despite these large strain-specific differences in colonization efficiency, overall bacterial colonization per fish correlated with number of bacteria in the water at the time of sampling (Fig. S8B; $R^2 = 0.69$, $p = 0.03^*$).

The addition of loperamide led to a measurable reduction or increase in larval zebrafish bacterial load for half of the assayed strains. Five strains were not quantifiably affected by loperamide in mono-colonized zebrafish in our assays: S2, S3, S4, S5, and S6. Colonization of larvae exposed to S1 *P. mosselii* or S10 *F. johnsoniae* was significantly reduced in the presence of loperamide at T0 and T1 but recovered to match DMSO-level colonization by T5 (Fig. 4B; $p < 0.05$). S7 *A. veronii* and S9 *Ochrobactrum tritici* bacterial load was reduced at all timepoints with loperamide treatment. One strain (S8 *Rhizobium* sp.) showed higher colonization only at T5 after loperamide treatment (Fig. 4B; $p < 0.05$). These strain-specific colonization changes due to loperamide confirm inhibition or promotion of bacteria in vivo, in addition to the host-exclusive effects of the molecule. A summary

of how loperamide affects in vitro growth and survival, and in vivo mono-colonization of all strains is detailed in Table 1.

Loperamide treatment induces expected dysbiosis in mix5-colonized gnotobiotic larval zebrafish

In order to evaluate how loperamide affects a multi-species bacterial community in vivo, germ-free zebrafish were colonized with an equal mix of strains S1, S3, S5, S6, and S7. These strains were selected according to their varying sensitivities to loperamide in vitro and in vivo. Loperamide treatment did not lead to a measurable impact on the total number of CFUs per mix5-colonized fish (Fig. 5A). However, the addition of loperamide induced an increase in S7 *A. veronii* at T0, relative to the DMSO control (Fig. 5BC). Meanwhile, S3 and S5 increased in loperamide-treated samples at T1. Finally, at T5 after 5 days of recovery, S5 *S. maltophilia* and S7 *A. veronii* were the most abundant strains (Fig. 5BC). These changes in the proportion of each strain per fish reflect in vitro sensitivity to loperamide and changes measured in conventional fish during loperamide treatment.

Table 1 Summary of in vitro effects of loperamide on zebrafish strains. Significant changes in growth in media, survival in water, and in vivo zebrafish colonization for loperamide treated, compared to DMSO control

Strain	Growth in media	Survival in water	Zebrafish mono-colonization
S1. <i>Pseudomonas mosselii</i>	Promoted	No effect	Reduced at T0 and T1, and then recovery
S2. <i>Variovorax gossypii</i>	No effect	Increased from 6 h	No detected effect
S3. <i>Pseudomonas nitroreducens</i>	No effect	Increased from 24 h	No detected effect
S4. <i>Achromobacter marplatensis</i>	Reduced	No effect	No detected effect
S5. <i>Stenotrophomonas maltophilia</i>	Reduced	No effect	No detected effect
S6. <i>Aeromonas caviae</i>	Inhibited	No effect	No detected effect
S7. <i>Aeromonas veronii</i>	Inhibited	Decreased at 24 h	Reduced at T0 and T5
S8. <i>Rhizobium sp.</i>	Inhibited	Increased from 24 h	Increased at T5
S9. <i>Ochrobactrum tritici</i>	Inhibited	No effect	Reduced at T0
S10. <i>Flavobacterium johnsoniae</i>	Inhibited	No effect	Reduced at T0 and T1, and then recovery

Differences in strain-specific colonization efficiency in zebrafish individually colonized with these 5 strains may have contributed to loperamide-independent effects on the mix5-bacterial colonization (Fig. S8). We compared the mix5-colonized bacterial composition with the sum of mono-colonized bacterial abundances for S1, S3, S5, S6, and S7 (Fig. S9). This comparison of the mono means to the mix5 showed that the composition of the mix5-colonized fish was different from the sum of the mono-colonized fish in all conditions (Fig. S9AB). Therefore, inter-bacterial competition in the mix5-colonized fish also contributed to changes in community composition, in addition to host selection and bacterial inhibition by loperamide. Comparison of the CFUs per strain in mono-colonized fish to mix5-colonized fish also showed increased colonization for each strain in mono—than when part of a mix, regardless of timepoint or treatment and despite the increased number of bacteria added (Fig. S9C, D). Even in control conditions, each strain colonized 10–10,000 times higher when added alone than when added as part of a mix (Fig. S9C, D).

Further comparison of the bacterial composition in conventional and gnotobiotic zebrafish focused on changes in alpha diversity after loperamide treatment and during recovery. Loperamide-treated conventional fish alpha diversity measured by Simpson's index and evenness significantly decreased after 24 h of loperamide treatment (T0; $p < 0.05$), then increased after 24 h of recovery (T1), and stayed similar to control diversity at T5 days post-treatment (Fig. 6AC). This decrease in Simpson's diversity is reflected in the lower number of ASVs (richness) detected in the loperamide-treated samples at T0 (Fig. S1B, first panel). Similarly, the alpha diversity of loperamide-treated mix5-colonized gnotobiotic zebrafish decreased at T0, significantly increased at T1 ($p < 0.05$), and recovered to match the control at T5

(Fig. 6D). Observed richness did not significantly change in the conventional or gnotobiotic models (Fig. 6BE), indicating that the changes in Simpson's index are not due to a change in the number of strains or taxa per fish. These results show that in both natural and synthetic zebrafish bacterial communities, loperamide induced a significant, but recoverable, dysbiosis and associated loss in diversity.

Discussion

Understanding the impact of nonantibiotic drugs on host-associated microbiota is critical for sustaining health in humans as well as animal models. In this study, we evaluated the effects of loperamide, a widely prescribed anti-diarrheal compound also used as a tool to study the impact of bowel dysfunctions in animal models. Using conventional and gnotobiotic zebrafish, we showed that loperamide directly induced significant but recoverable dysbiosis by broad-range inhibition. The effects of loperamide on zebrafish-associated bacteria characterized by growth, survival, and colonization capacity were strain specific and changed in the presence of other bacteria or the zebrafish host.

Loperamide induced decreases in microbiota alpha diversity and beta dispersion immediately after loperamide treatment. These changes were not permanent, and initial alpha diversity recovered within 24 h after loperamide exposition and within 5 days for beta diversity. These results were consistent with a previous study in mice, in which loperamide was used to increase gastrointestinal transit time but also led to alterations in the gut microbial community that were reversible after treatment interruption [59]. This dysbiosis was presumed to result from a reduction of peristaltic movement, but our results suggest that it could also be explained by the loperamide bactericidal activity [27, 28].

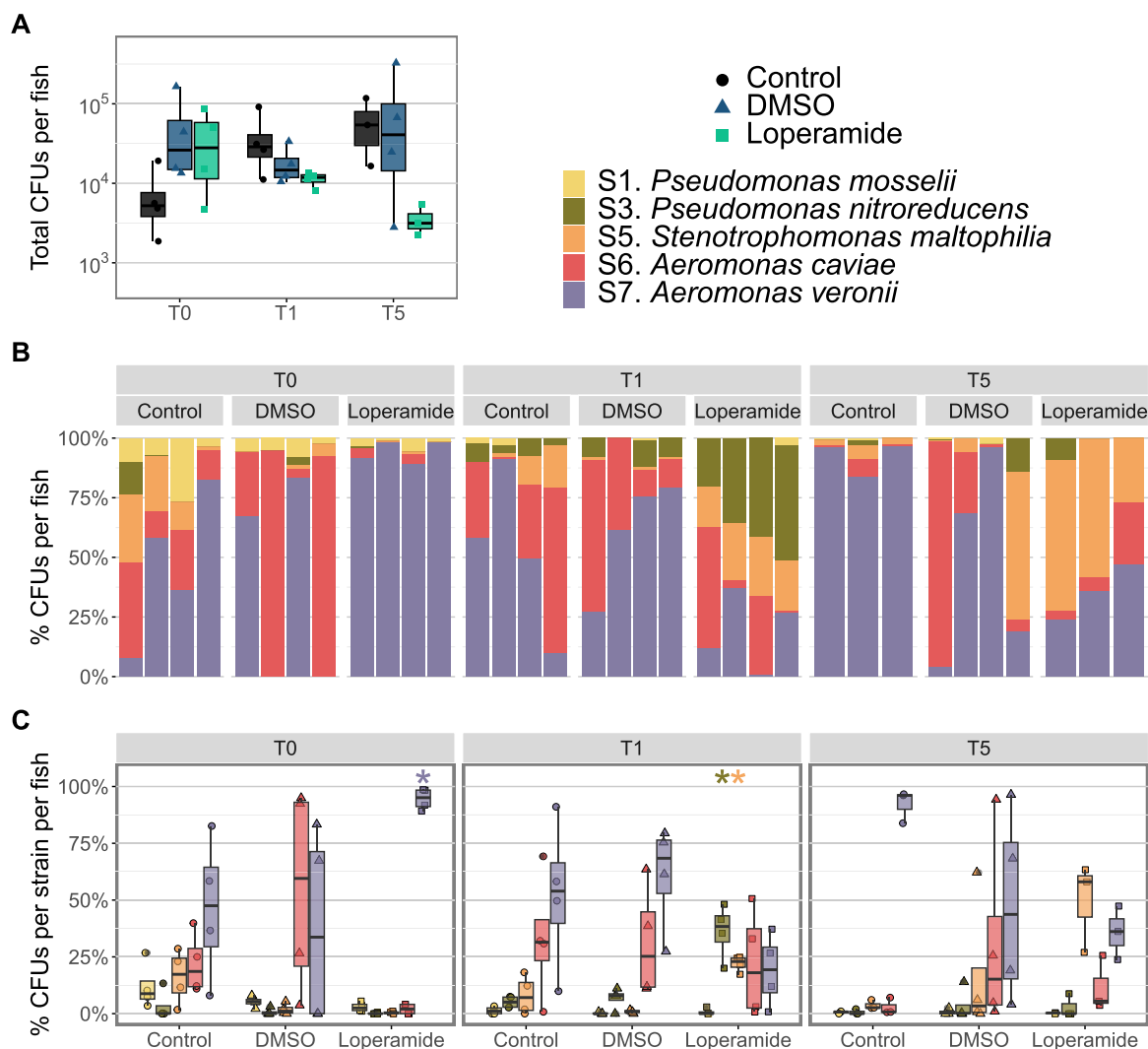


Fig. 5 Loperamide affects mix5-colonized gnotobiotic zebrafish bacterial load and composition. **A** Total CFUs per fish of mix5-colonized fish after exposure to loperamide at 3 timepoints ($n=3-4$ fish). Each point represents a single zebrafish (mean of 3 technical replicates). No significant changes were found for loperamide treatment, compared to DMSO. Wilcoxon test. Note log scale for CFUs. **B** Percent abundance of each strain per mix5-colonized fish. Each bar is an individual fish sample. **C** Percent abundance of each strain in mix5-colonized fish per timepoint and treatment. Each point represents a single zebrafish (mean of 3 technical replicates). * $p < 0.05$ for loperamide treatment, compared to DMSO. Wilcoxon test

We found that the effects of loperamide treatment on zebrafish microbiota composition depended on a strain’s survival in water and colonization capacity. In conventional zebrafish, loperamide induced a significant increase in the *Aeromonas* genus at T0, but not at T1 or T5. In mono-colonized fish, S6 *A. caviae* was not affected by loperamide, but S7 *A. veronii* showed impaired colonization despite its high colonization efficiency. S7 *A. veronii* was the only strain with inhibited growth and decreased survival in water over time, which may have contributed to its inability to recover colonization capacity after loperamide treatment. In the mix5-colonized

fish, S7 *A. veronii* was the most abundant strain in the loperamide-treated zebrafish at T0, but significantly decreased at T1 and T5, consistent with its colonization in the mono-colonized larvae and the conventional zebrafish composition. Other bacteria- or host-related factors induced by the presence of loperamide could explain reduced S7 *A. veronii* abundance, such as reduced feeding, chemokinesis, or motility [22, 60, 61]. Previous studies of gnotobiotic zebrafish colonization have demonstrated the strain-specific importance of chemotaxis and host gut motility for intestinal colonization [62, 63], bacterial motility and host cues with *A. veronii* [61], and

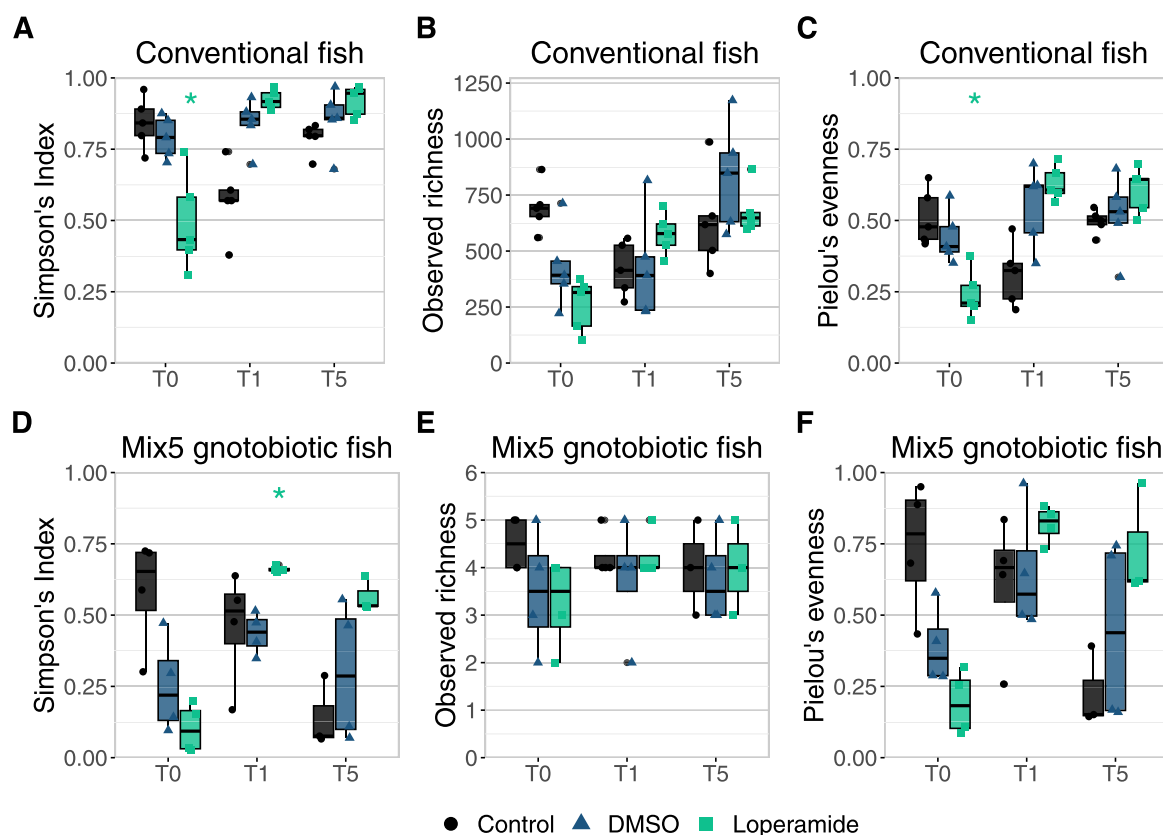


Fig. 6 Simpson's diversity of conventional and gnotobiotic zebrafish decreases but recovers after loperamide treatment. Alpha-diversity indices calculated at each timepoint for control water, DMSO, and loperamide-treated samples for **A–C** 16S rRNA gene amplicon data at the ASV level in conventional fish ($n=5$ fish) and **D–F** CFUs per strain in mix5-colonized fish ($n=3–4$ fish). **A** and **D** Simpson's index (H). **B** and **E** Observed richness (S_{obs}) and **C** and **F** Pielou's evenness ($H/\log(S_{obs})$) are shown. Each point represents a single zebrafish with boxplots shown per condition. * $p < 0.05$ for loperamide treatment, compared to DMSO. Wilcoxon test

general induction of host immune responses or locomotive behavior [64–66]. In a mix5-colonized community, bacteria-bacteria interactions also contribute to changes in relative abundance, regardless of host factors. For example, the ecological niche left by S7 *A. veronii* due to direct inhibition or decreased intestinal peristalsis from loperamide treatment could explain why S3 *P. nitroreducens* showed a significant increase at T1 only in loperamide-treated samples.

Interestingly, loperamide did not increase bacterial load at the measured timepoints in our study. Similar results were also obtained in loperamide-induced constipation model in rats [67]. This may be due to colonization constraints imposed by loperamide toxicity, the larval fish size, or nutrient limitations, since previous studies of gnotobiotic zebrafish have also not detected more than 10^6 CFUs/larvae [22, 64, 65]. Our study is limited to bulk culturable CFUs per fish associated with 10 bacterial strains at 3 timepoints. Future studies should investigate the localization and quantification of transit time of fluorescently tagged bacteria to further

understand intestinal-specific changes upon loperamide treatment.

In all previous studies where loperamide-induced constipation has been considered to affect the host microbiome, these changes have been attributed to decreased stool frequency and increased colonic contractions by inhibition of intestinal water secretion and colonic peristalsis, which extends the fecal evacuation time and delays the intestinal luminal transit rate [15, 68]. However, our results demonstrated that the changes in microbiota composition and diversity are also partially due to strain-specific bacterial inhibition or promotion by the loperamide exposure. In addition to the zebrafish-associated strains studied here, loperamide exhibits bactericidal activity against diverse host-associated microbes including mycobacterial strains (e.g., *Mycobacterium tuberculosis*) and *Staphylococcus aureus*, but not *Escherichia coli* [27, 69]. These microbes are members of the human and vertebrate microbiome that may be directly affected by loperamide treatment, resulting in unforeseen microbiota modulation [70].

Prior studies of loperamide-induced gastrointestinal disorders determined that various treatments restore host health and improve the associated symptoms (i.e., constipation or gut transit time). For example, konjac oligo-glucomannan alleviates defecation infrequency and suppressed the growth of *Bacteroides* in mice [71], raffinose-oligosaccharide improved gastrointestinal transit rate and reduced the serum levels of vasoactive intestinal peptide in mice [72], and probiotics improved constipation by altering metabolite, amino acid, inflammatory cytokines, and/or neurotransmitter abundances in rats [20, 73, 74]. In all of these studies, the effect of treatment and changes in host physiology were inferred to constipation or the relevant model phenotype. However, all of these described effects may also be attributed to ancillary microbiota modulations. The perturbation of host microbiomes is frequently described to cause significant changes in host metabolite and peptide abundances, immune response, and physiology and health [1, 75, 76]. Our results indicate that animal models using loperamide to study bowel dysfunction and constipation cannot distinguish the effects of loperamide on host function from the effects of microbiota modulation by loperamide.

Conclusions

In summary, our results demonstrate that loperamide induces significant changes in the microbiota, which may influence experimental outcomes especially if the host immune system or behavior is considered. As a common medication used to alleviate diarrhea and bowel disorders in humans, loperamide is also likely to produce understudied antibiotic effects on intestinal microbiota. This emphasizes the need to better characterize relationships between host physiological changes, microbial community structure, and disease or dysbiosis states.

Supplementary Information

The online version contains supplementary material available at <https://doi.org/10.1186/s40168-023-01690-z>.

Additional file 1: Supplementary figures: Fig. S1. Sequencing depth and coverage for 16S rRNA gene amplicon data from conventional zebrafish larvae. (A) Number of quality-controlled bacterial sequences per sample. (B). ASV rarefaction curves of all zebrafish larvae samples separated by timepoint and colored by treatment group ($n = 5$ fish per condition). **Fig. S2.** Controls for 16S rRNA amplicon sequencing data: blanks and mock community. (A) Expected mock abundance of ASVs for each negative sequencing control sample: Zymo mock community standard D6305 (Mock_1 and Mock_2). (C) Relative percent abundance of ASVs for each negative sequencing control sample: negative DNA extraction (Neg_kit1 and Neg_kit2) and negative PCR amplification (Neg_PCR1). The top 10 most abundant ASVs are shown, with all others grouped in the grey "Others" category. **Fig. S3.** 16S rRNA gene amplicon relative abundances at the phylum level. (A) Bar plot of percent phylum abundance per sample. The top 8 most abundant phyla are shown with the others grouped

into "Others" ($n = 5$ fish per condition). **Fig. S4.** 16S rRNA gene amplicon relative abundances at the genus level. (A) Bar plot of percent genus abundance per sample. The top 12 most abundant genera are shown with the others grouped into "Others" ($n = 5$ fish per condition). (B) Number of bacterial genera shared between DMSO and Loperamide-treated samples at each timepoint (vertical bars). The total number of genera detected in each group is shown in the horizontal bar plot on the right. **Fig. S5.** Beta-diversity metrics of 16S rRNA gene amplicons sequenced from conventional zebrafish. (A) NMDS plot calculated using Bray-Curtis beta-diversity ($k=2$) of percent normalized ASVs from 16S rRNA gene amplicons for all water control, DMSO control, and loperamide-treated samples. Ellipse lines show the 95 % confidence interval (standard deviation). Stress = 0.139 ($n = 5$ fish per condition). (B-D) NMDS plot calculated using Bray-Curtis beta-diversity ($k=2$) of percent normalized ASVs from 16S rRNA gene amplicons at each timepoint (B) T0 6 dpf (adonis2 PERMANOVA $R^2 = 0.43$; $p < 0.01$), (C) T1 7 dpf (adonis2 PERMANOVA $R^2 = 0.51$; $p < 0.01$), and (D) T5 11 dpf (adonis2 PERMANOVA $R^2 = 0.22$; $p > 0.05$). The stress in indicated on each plot. (E) Beta-dispersion or within-condition dissimilarity index calculated using Bray-Curtis beta-diversity ($n = 15$; 3 treatment groups for each of 5 samples per condition). **** $p < 0.001$ for Loperamide-treatment, compared to DMSO. Wilcoxon test. **Fig. S6.** Growth parameters measured for zebrafish larvae. (A) Fish length, (B) rump length, (C) tail width, and (D) eye diameter measurements of larval zebrafish at 6 dpf, 7 dpf, and 11 dpf (T0, T1, T5 after 24-hour treatment). All measurements are shown in millimeters ($n = 10$ fish per condition). * $p < 0.05$ for Loperamide treatment, compared to DMSO. Wilcoxon test. The only significant difference is in (D) Eye diameter at T5. (E) Example fish image with the four measurements indicated and scale bar. **Fig. S7.** Growth curves of zebrafish-associated bacterial strains exposed to loperamide. Growth curves of 10 strains isolated from the fish environment or environmental *Flavobacterium* spp. (additional strain details are in Table S1). The thick line represents the mean of all biological replicates ($n=3-8$). Each thin line represents a biological replicate (mean of 3 technical replicates). Every condition was repeated at least twice. **Fig. S8.** Comparison of bacterial load in water and zebrafish mono-colonization capacity in control conditions. (A) Boxplots showing CFUs per mL in water at 48 h and CFUs per fish at T0 (6 dpf) for each of the 10 bacterial strains ordered by colonization efficiency. The value indicated on the plot is the colonization efficiency, calculated by Colonization efficiency = CFUs per Fish / Water CFUs per mL * 100. Note log scale on axis. (B) Correlation between bacterial load in water with zebrafish colonization efficiency. The grey dotted line indicates the 1:1 line. The regression line is indicated by the solid black line and the fitted equation, R^2 and p -value are shown in the top left corner. The strains with the lowest (S8) and the highest (S7) colonization efficiency are highlighted. **Fig. S9.** Comparison of mono-colonized means with mix5-colonized fish. (A) Mix5-colonized means per condition and timepoint normalized to percent CFUs per fish. (B) Mono-colonized fish means combined as a hypothetical mix per condition and timepoint, normalized to percent CFUs per condition. (C) Mix5-colonized means per condition and timepoint as CFUs per fish per strain. (D) Mono-colonized fish CFUs per fish per strain. For C and D: mean \pm standard deviation per condition is shown on log scale ($n = 3-4$ fish). **Table S1.** Zebrafish environment bacterial strains used in this study

Acknowledgements

We are grateful to Jean-Pierre Levraud, Yulixis Ramayo, and Erin Witkop for critical reading of the manuscript. The graphical abstract and Figure 1 were created with BioRender.com.

Authors' contributions

RJS, JMG and DPP contributed to the conception and design of the study. RJS, DPP and BA performed the experiments. SB and ND performed the zebrafish imaging assay. RJS analyzed the data and wrote the first draft of the manuscript. All authors contributed to manuscript revision, read and approved the submitted version.

Authors' information

Not applicable.

Funding

This work was supported by grants from the French Government's Investissement d'Avenir program, Laboratoire d'Excellence "Integrative Biology of Emerging Infectious Diseases" (grant n°ANR-10-LABX-62-IBEID), and by the Fondation pour la Recherche Médicale (grant DEQ20180339185). R. J. S. was supported by a grant from the Philippe Foundation. Sequencing was performed by G. M. Haustant, L. Lemée, Biomix Platform, C2RT, Institut Pasteur, Paris, France, supported by France Génomique (ANR-10-INBS-09-09) and IBISA.

Availability of data and materials

The raw 16S rRNA gene amplicon sequences generated for this study can be found in the NCBI Sequencing Read Archive in BioProject no. PRJNA908751. All other raw data, processed sequencing files, QIIME2 artifacts, and scripts to reproduce the figures in the manuscript are available in the Zenodo repository, <https://doi.org/10.5281/zenodo.8152593> [48].

Declarations

Ethics approval and consent to participate

All animal experiments described in the present study were conducted at the Institut Pasteur according to the European Union directive 2010/63/EU and authorized by the Institut Pasteur Animal Health and Care Committees under permit no. dap220109.

Consent for publication

Not applicable.

Competing interests

The authors declare no competing interests.

Author details

¹Genetics of Biofilms Laboratory, UMR 6047, Institut Pasteur Université Paris Cité, CNRS, Paris, France. ²Zebrafish Neurogenetics Laboratory, UMR 3738, Institut Pasteur Université Paris Cité, CNRS, Paris, France.

Received: 18 April 2023 Accepted: 4 October 2023

Published online: 11 November 2023

References

- Hill JH, Round JL. Snapshot: microbiota effects on host physiology. *Cell*. 2021;184:2796-2796.e1.
- Obeng N, Bansept F, Sieber M, Traulsen A, Schulenburg H. Evolution of microbiota–host associations: the microbe's perspective. *Trends in Microbiology*. 2021;:1–9.
- Libertucci J, Young VB. The role of the microbiota in infectious diseases. *Nat Microbiol*. 2019;4:35–45.
- Henry LP, Bruijning M, Forsberg SKG, Ayroles JF. The microbiome extends host evolutionary potential. *Nat Commun*. 2021;12:1–13.
- Wilkins LGE, Leray M, O'Dea A, Yuen B, Peixoto R, Pereira TJ, et al. Host-associated microbiomes drive structure and function of marine ecosystems. *PLoS Biol*. 2019;17:e3000533.
- Stecher B, Maier L, Hardt WD. "Blooming" in the gut: how dysbiosis might contribute to pathogen evolution. *Nat Rev Microbiol*. 2013;11:277–84.
- Hooks KB, O'Malley MA. Dysbiosis and its discontents. *mBio*. 2017;8.
- Douglas AE. Simple animal models for microbiome research. *Nat Rev Microbiol*. 2019;17:764–75.
- Clavel T, Lagkouvardos I, Stecher B. From complex gut communities to minimal microbiomes via cultivation. *Curr Opin Microbiol*. 2017;38:148–55.
- Mooser C, Gomez de Agüero M, Ganal-Vonarburg SC. Standardization in host–microbiota interaction studies: challenges, gnotobiology as a tool, and perspective. *Curr Opin Microbiol*. 2018;44:50–60.
- Stagaman K, Sharpton TJ, Guillemin K. Zebrafish microbiome studies make waves. *Lab Anim*. 2020;49:201–7.
- Zhang M, Shan C, Tan F, Limbu SM, Chen L, Du ZY. Gnotobiotic models: powerful tools for deeply understanding intestinal microbiota–host interactions in aquaculture. *Aquaculture*. 2020;517:734800.
- Pham LN, Kanther M, Semova I, Rawls JF. Methods for generating and colonizing gnotobiotic zebrafish. *Nat Protoc*. 2008;3:1862–75.
- Milligan-Myhre K, Charette JR, Phennicie RT, Stephens WZ, Rawls JF, Guillemain K, et al. Study of host–microbe interactions in zebrafish. In: *Methods in Cell Biology*. Academic Press Inc.; 2011. p. 87–116.
- Awouters F, Megens A, Verlinden M, Schuurkes J, Niemegeers C, Janssen PAJ. Loperamide. *Dig Dis Sci*. 1993;38:977–95.
- Baldi F, Bianco MA, Nardone G, Pilotto A, Zamparo E. Focus on acute diarrhoeal disease. *World J Gastroenterol*. 2009;15:3341–8.
- Diemert DJ. Prevention and self-treatment of traveler's diarrhea. *Clin Microbiol Rev*. 2006;19:583–94.
- Li STT, Grossman DC, Cummings P. Loperamide therapy for acute diarrhea in children: systematic review and meta-analysis. *PLoS Med*. 2007;4:495–505.
- Touw K, Wang Y, Leone V, Nadimpalli A, Nathaniel H, Gianrico F, et al. Drug-induced constipation alters gut microbiota stability leading to physiological changes in the host. *The FASEB Journal*. 2014;28 1 Supplement.
- Inatomi T, Honma M. Effects of probiotics on loperamide-induced constipation in rats. *Sci Rep*. 2021;11:1–9.
- Shi Y, Zhang Y, Zhao F, Ruan H, Huang H, Luo L, et al. Acetylcholine serves as a derepressor in loperamide-induced opioid-induced bowel dysfunction (OIBD) in zebrafish. *Sci Rep*. 2014;4:1–12.
- Lu Y, Zhang J, Yi H, Zhang Z, Zhang L. Screening of intestinal peristalsis-promoting probiotics based on a zebrafish model. *Food Funct*. 2019;10:2075–82.
- Yang L, Wan Y, Li W, Liu C, Li HF, Dong Z, et al. Targeting intestinal flora and its metabolism to explore the laxative effects of rhubarb. *Appl Microbiol Biotechnol*. 2022;106:1615–31.
- Touw K, Ringus DL, Hubert N, Wang Y, Leone VA, Nadimpalli A, et al. Mutual reinforcement of pathophysiological host–microbe interactions in intestinal stasis models. *Physiol Rep*. 2017;5:e13182.
- Wang G, Yang S, Sun S, Si Q, Wang L, Zhang Q, et al. Lactobacillus rhamnosus strains relieve loperamide-induced constipation via different pathways independent of short-chain fatty acids. *Front Cell Infect Microbiol*. 2020;10:423.
- Hwang N, Eom T, Gupta SK, Jeong SY, Jeong DY, Kim YS, et al. Genes and gut bacteria involved in luminal butyrate reduction caused by diet and loperamide. *Genes*. 2017;8:1–12.
- Barrientos OM, Juárez E, Gonzalez Y, Castro-Villeda DA, Torres M, Guzmán-Beltrán S. Loperamide exerts a direct bactericidal effect against *M. tuberculosis*, *M. bovis*, *M. terrae* and *M. smegmatis*. *Lett Appl Microbiol*. 2021;72:351–6.
- Juárez E, Ruiz A, Cortez O, Sada E, Torres M. Antimicrobial and immunomodulatory activity induced by loperamide in mycobacterial infections. *Int Immunopharmacol*. 2018;65:29–36.
- Maier L, Pruteanu M, Kuhn M, Zeller G, Telzerow A, Anderson EE, et al. Extensive impact of non-antibiotic drugs on human gut bacteria. *Nature*. 2018;555:623–8.
- Rendueles O, Ferrières L, Frétaud M, Bégaud E, Herbomel P, Levraud JP, et al. A new zebrafish model of oro-intestinal pathogen colonization reveals a key role for adhesion in protection by probiotic bacteria. *PLoS Pathog*. 2012;8:12.
- Eren AM, Vineis JH, Morrison HG, Sogin ML. A filtering method to generate high quality short reads using illumina paired-end technology. *PLoS ONE*. 2013;8:e66643.
- Huse SM, Mark Welch DB, Voorhis A, Shipunova A, Morrison HG, Eren AM, et al. VAMPS: a website for visualization and analysis of microbial population structures. *BMC Bioinformatics*. 2014;15:41.
- Callahan BJ, McMurdie PJ, Rosen MJ, Han AW, Johnson AJA, Holmes SP. DADA2: high-resolution sample inference from illumina amplicon data. *Nat Methods*. 2016;13:581–3.
- Caporaso JG, Kuczynski J, Stombaugh J, Bittinger K, Bushman FD, Costello EK, et al. QIIME allows analysis of high-throughput community sequencing data. *Nat Methods*. 2010;7:335–6.
- Bokulich NA, Kaehler BD, Rideout JR, Dillon M, Bolyen E, Knight R, et al. Optimizing taxonomic classification of marker-gene amplicon sequences with QIIME 2's q2-feature-classifier plugin. *Microbiome*. 2018;6:90.
- Bolyen E, Rideout JR, Dillon MR, Bokulich NA, Abnet CC, Al-Ghalith GA, et al. Reproducible, interactive, scalable and extensible microbiome data science using QIIME 2. *Nat Biotechnol*. 2019;37:852–7.

37. Dixon P. VEGAN, a package of R functions for community ecology. *J Veg Sci.* 2003;14:927–30.
38. McMurdie PJ, Holmes S. Phyloseq: an R package for reproducible interactive analysis and graphics of microbiome census data. *PLoS ONE.* 2013;8:e61217.
39. Wickham H, Averick M, Bryan J, Chang W, McGowan L, François R, et al. Welcome to the Tidyverse. *Journal of Open Source Software.* 2019;4:1686.
40. Chao A, Jost L. Coverage-based rarefaction and extrapolation: standardizing samples by completeness rather than size. *Ecology.* 2012;93:2533–47.
41. Mcardle BH, Anderson MJ. Fitting multivariate models to community data : a comment on distance-based redundancy analysis published by : Ecological Society of America Stable URL : <http://www.jstor.org/stable/2680104>. *Ecology.* 2010;82:290–7.
42. Warton DI, Wright ST, Wang Y. Distance-based multivariate analyses confound location and dispersion effects. *Methods Ecol Evol.* 2012;3:89–101.
43. Law CW, Chen Y, Shi W, Smyth GK. Voom: precision weights unlock linear model analysis tools for RNA-seq read counts. *Genome Biol.* 2014;15:1–17.
44. Ritchie ME, Phipson B, Wu D, Hu Y, Law CW, Shi W, et al. Limma powers differential expression analyses for RNA-sequencing and microarray studies. *Nucleic Acids Res.* 2015;43:e47.
45. Cao Y. microbiomeMarker: microbiome biomarker analysis. 2020.
46. Gu Z, Eils R, Schlesner M. Complex heatmaps reveal patterns and correlations in multidimensional genomic data. *Bioinformatics.* 2016;32:2847–9.
47. Conway JR, Lex A, Gehlenborg N. UpSetR: an R package for the visualization of intersecting sets and their properties. *Bioinformatics.* 2017;33:2938–40.
48. Stevick R. Analyses for anti-diarrheal drug loperamide induces microbial dysbiosis in larval zebrafish via targeted bacterial inhibition. 2022. Zenodo. <https://doi.org/10.5281/zenodo.8152593>.
49. Schneider CA, Rasband WS, Eliceiri KW. NIH image to ImageJ: 25 years of image analysis. *Nat Methods.* 2012;9:671–5.
50. Parichy DM, Elizondo MR, Mills MG, Gordon TN, Engeszer RE. Normal table of postembryonic zebrafish development: staging by externally visible anatomy of the living fish. *Dev Dyn.* 2009;238:2975–3015.
51. Hinz C, Gebhardt K, Hartmann AK, Sigman L, Gerlach G. Influence of kinship and MHC class II genotype on visual traits in zebrafish larvae (*Danio rerio*). *PLoS ONE.* 2012;7(12):e51182.
52. Sales Cadena MR, Cadena PG, Watson MR, Sarmah S, Boehm SL, Marrs JA. Zebrafish (*Danio rerio*) larvae show behavioral and embryonic development defects when exposed to opioids at embryo stage. *Neurotoxicology and Teratology.* 2021;85 February.
53. Stressmann FA, Bernal-Bayard J, Perez-Pascual D, Audrain B, Rendueles O, Briolat V, et al. Mining zebrafish microbiota reveals key community-level resistance against fish pathogen infection. *ISME J.* 2021;15:702–19.
54. Perez-Pascual D, Vendrell-Fernandez S, Audrain B, Bernal-Bayard J, Patiño-Navarrete R, Petit V, et al. Gnotobiotic rainbow trout (*Oncorhynchus mykiss*) model reveals endogenous bacteria that protect against *Flavobacterium columnare* infection. *PLoS Pathog.* 2021;17:1–21.
55. Yoon SH, Ha SM, Kwon S, Lim J, Kim Y, Seo H, Chun J. Introducing EzBioCloud: A taxonomically united database of 16S rRNA and whole genome assemblies. *Int J Syst Evol Microbiol.* 2017;67:1613–7.
56. Kassambara A. ggpubr: “ggplot2” based publication ready plots. 2020.
57. Pedersen TL. Patchwork: the composer of plots. 2020.
58. Wilke CO. ggtext: improved text rendering support for “ggplot2.” 2020.
59. Kashyap PC, Marcobal A, Ursell LK, Larauche M, Duboc H, Earle KA, et al. Complex interactions among diet, gastrointestinal transit, and gut microbiota in humanized mice. *Gastroenterology.* 2013;144:967–77.
60. Lebov JF, Schlomann BH, Robinson CD, Bohannan BJM. Phenotypic parallelism during experimental adaptation of a free-living bacterium to the zebrafish gut. *mBio.* 2020;11:1–17.
61. Robinson CD, Sweeney EG, Ngo J, Remington SJ, Bohannan BJM, Robinson CD, et al. Host-emitted amino acid cues regulate bacterial chemokinesis to enhance colonization. *Cell Host and Microbe.* 2021;11–14.
62. Stephens WZ, Wiles TJ, Martinez ES, Jemielita M, Burns AR, Parthasarathy R, et al. Identification of population bottlenecks and colonization factors during assembly of bacterial communities within the zebrafish intestine. *mBio.* 2015;6:1–11.
63. Wiles TJ, Jemielita M, Baker RP, Schlomann BH, Logan SL, Ganz J, et al. Host gut motility promotes competitive exclusion within a model intestinal microbiota. *PLoS Biol.* 2016;14:1–24.
64. Wiles TJ, Schlomann BH, Wall ES, Betancourt R, Parthasarathy R, Guillemin K. Swimming motility of a gut bacterial symbiont promotes resistance to intestinal expulsion and enhances inflammation. *PLoS Biol.* 2020;18:e3000661.
65. Weitekamp CA, Kvasnicka A, Keely SP, Brinkman NE, Howey XM, Gaballah S, et al. Monoassociation with bacterial isolates reveals the role of colonization, community complexity and abundance on locomotor behavior in larval zebrafish. *Animal Microbiome.* 2021;3:12.
66. Tan F, Limbu SM, Qian Y, Qiao F, Du ZY, Zhang M. The responses of germ-free zebrafish (*Danio rerio*) to varying bacterial concentrations, colonization time points, and exposure duration. *Front Microbiol.* 2019;10:2156.
67. Kim J-E, Choi Y-J, Lee S-J, Gong J-E, Jin Y-J, Park S-H, et al. Laxative effects of phlorotannins derived from *Ecklonia cava* on loperamide-induced constipation in SD rats. *Molecules.* 2021;26:7209.
68. Schiller LR, Santa Ana CA, Morawski SG, Fordtran JS. Mechanism of the anti-diarrheal effect of loperamide. *Gastroenterology.* 1984;86:1475–80.
69. Chai CLL, Teo SLM, Jameson FKM, Lee SSC, Likhitsup A, Chen C-L, et al. Loperamide-based compounds as additives for biofouling management. *Scopus.* 2014.
70. Huttenhower C, Human Microbiome Project Consortium. Structure, function and diversity of the healthy human microbiome. *Nature.* 2012;486:207–14.
71. Hayeeawaema F, Wichienchot S, Khuittuan P. Amelioration of gut dysbiosis and gastrointestinal motility by konjac oligo-glucomannan on loperamide-induced constipation in mice. *Nutrition.* 2020;73:110715.
72. Liang Y, Wang Y, Wen P, Chen Y, Ouyang D, Wang D, et al. The anti-constipation effects of raffinose-oligosaccharide on gut function in mice using neurotransmitter analyses, 16S rRNA sequencing and targeted screening. *Molecules.* 2022;27(7):2235.
73. Eor JY, Tan PL, Lim SM, Choi DH, Yoon SM, Yang SY, et al. Laxative effect of probiotic chocolate on loperamide-induced constipation in rats. *Food Res Int.* 2019;116:1173–82.
74. Makizaki Y, Uemoto T, Yokota H, Yamamoto M, Tanaka Y, Ohno H. Improvement of loperamide-induced slow transit constipation by *Bifidobacterium bifidum* G9–1 is mediated by the correction of butyrate production and neurotransmitter profile due to improvement in dysbiosis. *PLoS One.* 2021;16(3):e0248584.
75. Fontaine SS, Kohl KD. Optimal integration between host physiology and functions of the gut microbiome. *Philos Trans R Soc B Biol Sci.* 2020;375:20190594.
76. Levy M, Blacher E, Elinav E. Microbiome, metabolites and host immunity. *Curr Opin Microbiol.* 2017;35:8–15.

Publisher's Note

Springer Nature remains neutral with regard to jurisdictional claims in published maps and institutional affiliations.

Ready to submit your research? Choose BMC and benefit from:

- fast, convenient online submission
- thorough peer review by experienced researchers in your field
- rapid publication on acceptance
- support for research data, including large and complex data types
- gold Open Access which fosters wider collaboration and increased citations
- maximum visibility for your research: over 100M website views per year

At BMC, research is always in progress.

Learn more biomedcentral.com/submissions

